

Theoretical study of reaction mechanisms for the ketonization of vinyl alcohol in gas phase and aqueous solution

**Oscar N. Ventura¹, Agustí Lledós², Rosanna Bonaccorsi³, Juan Bertrán²
and Jacopo Tomasi⁴**

¹ Cátedra de Química Cuántica, Facultad de Química, C.C. 1157, Montevideo, Uruguay

² Department de Química-Física, Facultat de Ciències, Universitat Autònoma de Barcelona, Bellaterra, Barcelona, Spain

³ Istituto di Chimica Quantistica ed Energetica Molecolare del C.N.R., Università di Pisa, Via Risorgimento 35, I-56100 Pisa, Italy

⁴ Dipartimento di Chimica e Chimica Industriale, Università di Pisa, Via Risorgimento 35, I-56100 Pisa, Italy

(Received 9 January; revised and accepted May 29, 1987)

Theoretical *ab initio* calculations are done on different mechanisms for the conversion of vinyl alcohol to acetaldehyde, both in gas phase and in solution. Several basis sets are used in order to assess the accuracy of the results in gas phase and a continuum model of the solvent is employed to mimic reactions in water solution. The results indicate a catalytic action of water in hydrated clusters in gas phase, whereas in solution, and within the error limits of our calculations, both neutral water-chain and ionic mechanisms appear to be equally probable. Finally, the action of acids or bases is tested through the analysis of the reaction of vinyl alcohol with H_3O^+ and HO^- . The results of the calculations are shown to be in qualitative agreement with the experimental facts when 6-31++G basis set is used but not when either STO-3G or 4-31G basis sets are employed.

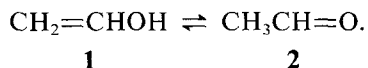
Key words: Vinyl alcohol — Keto-enolic tautomerism — *Ab initio* methods — Solvation energy

1. Introduction

Prototropic reactions are good examples of chemical interactions where the intervention of the solvent may be crucial to the fate of the transformation.

Several theoretical studies of these processes have been published by now [1], showing clearly the qualitative differences between reactions where solvent molecules were included as part of the reacting system and those where they were not. These works, however, were concerned with molecular clusters more akin to gas-phase reactions than to processes in solution. In fact, the effect of surrounding bulk solvent was not taken into account in those studies and, consequently, processes like general-acid and general-base catalysis, important in solution, have not been considered. Use of continuum [2] and discrete [3] models of the solvent showed already the importance of that influence to stabilize ions and ionic pairs in solution. Therefore, we become interested in the study of cluster-type and ionic mechanisms for the aforementioned reactions using theoretical methods which mimic bulk solvent behavior.

In this paper we report a comparative study on the reaction of ketonization of vinyl alcohol, **1**, to acetaldehyde, **2**, in water solution through ionic and non-ionic mechanisms



A previous study of this keto-enolic tautomerism using gas-phase hydrated clusters [1a] was used as starting point for the work reported here. References to former work in the subject are given there.

2. The chemical problem

That keto forms of simple aldehydes and ketones are considerably more stable than the corresponding enols has been known for a long time [4]. However, the concept that enols, even simple ones, can be quite long-lived if they are generated in a manner that slows down the proton-transfer mechanisms of ketonization seems to be a more recent idea.

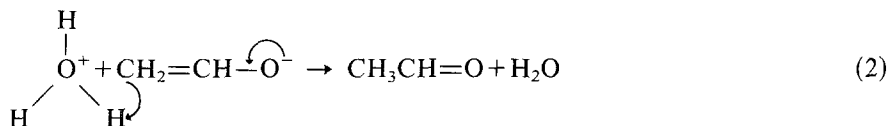
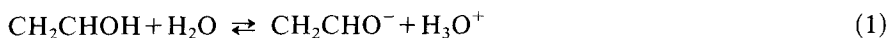
Vinyl alcohol, the enol tautomer of acetaldehyde, was only recently prepared. Saito [5] did it for the first time in 1976 by dehydration of ethylene glycol at 0.02–0.04 Torr and 900°C, and he found that **1** had a half-life of about 30 min in a Pyrex flask.

In solution things are slightly different. Blanck et al. [6] generated vinyl alcohol by irradiation of acetaldehyde or acetoin in a CIDNP experiment, finding a lifetime of about 25 s for this molecule. However, if a little *p*-Toluen sulphonic acid was added to the solution, thus catalyzing ketonization, vinyl alcohol could not be detected. Furthermore, Capon et al. [7] succeeded in preparing it in aqueous solution and made an estimation of 6.66 to 6.44 of pK_{enol} at 25°C (in agreement with the estimate of Guthrie et al. [8], $K_{\text{enol}} = 5 \times 10^{-6}$). This implies that very little vinyl alcohol is present in equilibrium conditions.

In accordance with the mechanisms of general keto-enolic tautomerism [4], conversion of vinyl alcohol to acetaldehyde is catalyzed by general acids and bases [7]. Capon et al. determined that acid-catalyzed ketonization was produced

by concerted protonation of the double bond by the acid catalyst and removal of the enolic proton by water acting as a general base. Base catalysis, on the other side, was explained by a mechanism involving rate-limiting C-protonation of the enolate anion.

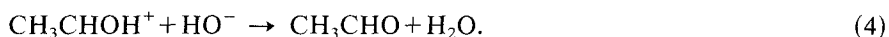
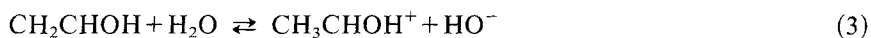
The experimental facts showed also [7] that vinyl alcohol undergoes a water-catalyzed or spontaneous ketonization with $k_{\text{H}_2\text{O}} = 1.38 \times 10^{-2} \text{ s}^{-1}$ at 15°C. Capon et al. [7] suggested the mechanism



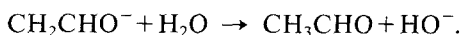
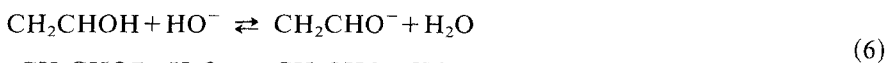
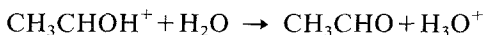
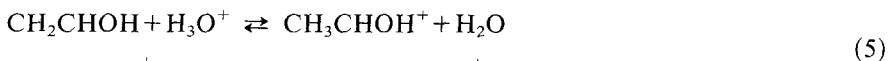
as suited to explain the experimental results, but did not rule out either a concerted mechanism or one where the equilibrium (1) is not reached because enolate and hydronium ion collapse faster to acetaldehyde than they diffuse apart.

In [1a] we reported on the drastic reduction of the potential energy barrier of that same reaction when a pair of water molecules intervened in a concerted fashion to facilitate proton transfer. In fact, the STO-3G value of 91.9 kcal/mol found for the sigmatropic 1,3-proton migration was reduced to 21.8 kcal/mol due to water intervention. This calculated barrier is, however, still too high to explain the observed rate of conversion in solution. Consequently, a closer look at the reaction seems adequate in order to investigate whether the theoretical results agree with the experimental facts.

In this paper we study the concerted water-chain mechanism using a better basis set than in [1a] and including the effects of bulk solvent by a continuum model. This mechanism is compared with both the one proposed by Capon et al. [7] (reactions (1) and (2)) and with the alternative mechanism of slow protonation at CH₂ of vinyl alcohol followed by fast deprotonation of oxygen in CH₃CHOH⁺ (reactions (3) and (4))



We studied also acid and base catalysis in this reaction, both in gas phase and in solution, through the mechanisms (5) and (6) respectively



The results obtained are compared with the water-chain and the ionic mechanisms in order to elucidate the fate of vinyl alcohol in water solution at the level given by the theoretical methods employed.

3. Methodology

3.1. Basis sets and geometry optimizations

Calculations reported in this paper were done using *ab initio* SCF methods. STO-3G [9] and 4-31G [10] basis sets were employed as a first approximation to the problem. However, it is known that theoretical investigations of anionic species, such as some of those considered in this paper, pose special problems [11] related to the fact that with commonly used basis sets the HOMO's of anions are often indicated erroneously to have positive energies. Chandrasekhar et al. [12] developed the 4-31+G basis set to cope with this problem, adding diffuse *sp* functions to the 4-31G set for first-row atoms. Using it to study proton affinities of some representative anions, they found that the average error was reduced from 38.3% (STO-3G) and 8.2% (4-31G) to an encouraging 2.8% (approximately 10 kcal/mol).

Regretfully, in a very interesting work published recently Cao et al. [13] showed that not even 4-31+G was able to give properly the energy of proton transfer in asymmetric systems. Since the processes we are studying belong to this category, we tried to select a slightly extended basis which hopefully could improve the results. It may be seen in [13] that the inappropriateness of 4-31+G basis set was due to the fact that it was better suited for anions than for neutral molecules. Thus, we chose the 6-311G basis set [14a], enlarged by diffuse *s*-gaussians on hydrogens and diffuse *sp*-functions on carbon and oxygen [12]. Some calculations, not reported here, convinced us that a triple-zeta valence basis set did not improve the results, and finally we used a 6-31++G basis set (6-31G [14b] augmented by *s*-gaussians on hydrogen and *sp*-functions on carbon and oxygen). Polarization functions were not included because our solvent modelling program is not able to treat them.

Using that 6-31++G set we calculated proton affinities of some of the molecules studied in this paper in order to compare them with other basis sets' results and with the experimental ones. These values are collected in Table 1. The 6-31++G proton affinities (PAs) were calculated using 4-31G optimized geometries, except for H₂O and H₃O⁺ where the planar and dihedral angles are badly given if no polarization functions are used [14c]. Thus, 6-31G* geometries from [13] were used in this case.

It is seen that the behavior of the 6-31++G set in this respect is similar to that of 4-31+G, with the possible exception that it improves the PAs of neutral systems more than this latter one with respect to the 4-31G set.

Using the values of Table 1 we calculated the energy for two of the asymmetric proton-transfer reactions on which we are interested, comparing the different basis sets used to obtain the PAs. They are given in Table 2.

Three conclusions may be tentatively reached from the few data of this table. First, that 4-31+G sometimes performed better (e.g. the first reaction) and sometimes worse (in the second one) than 4-31G basis set, as already remarked by Cao et al [13]. Second, that 6-31++G performs better than both 4-31G and

Table 1. Proton affinities of some species studied in this paper (in kcal/mol)

Species	4-31G//4-31G			4-31+G//4-31+G			6-31++G//4-31G			Exp. [Ref. ^a]
	PA	Δ^b	$\Delta\%^c$	PA	Δ^b	$\Delta\%^c$	PA	Δ^b	$\Delta\%^c$	
HO ⁻	426.0	35.2	8.2	394.6	3.8	1.0	393.9 ^f	3.1 ^f	0.8 ^f	390.8 [12]
H ₂ O	178.0	12.7	7.1	174.8	9.5	5.4	170.2 ^f	4.9 ^f	2.9 ^f	165.3 [12]
CH ₂ CHO ⁻		11.5	6.9		8.3	5.0		3.7 ^f	2.2 ^f	166.5 [15b]
CH ₃ CHO	391.6	25.2	6.4	374.5	8.1	2.2	375.5	9.1	2.4	366.4 [12]
	194.4	9.0	4.6				192.3	6.9	3.6	185.4 [15a]
		7.8	4.2					5.7	3.1	186.6 [15b]
Mean error		20.5 ^d	6.6 ^e		7.1 ^d	2.9 ^e		5.0 ^d	2.4 ^e	

^a Source of the experimental data^b Δ = PA (calculated) – PA (experimental), in kcal/mol^c $\Delta\%$ = 100 Δ /PA (experimental)^d $(\sum_i \Delta_i)/n$ ^e $(\sum_i \Delta\%_i)/n$ ^f 6-31++G//6-31G* values, see text**Table 2.** Energy of asymmetric proton transfers (in kcal/mol)

Reaction	(I) ^a	(II) ^b	(III) ^c	(IV) ^d
2H ₂ O → HO ⁻ + H ₃ O ⁺	242.8	216.6	218.9	225.5
CH ₂ CHOH + HO ⁻ → CH ₂ CHO ⁻ + H ₂ O	34.4	36.8	18.3	24.4
Mean Error	13.6	10.6	6.4	

^a (I) 4-31G//4-31G^b (II) 4-31+G//4-31+G^c (III) 6-31++G//4-31GH₂O and H₃O⁺ energies calculated using 6-31G* geometries^d (IV) Experimental; estimated as differences of proton affinities from Table 1**Table 3.** Total energies of some molecules studied in this work (in a.u.)

Molecule	6-31++G//4-31G	6-31++G//6-31G*	6-31++G//6-31++G
HO ⁻	-75.36440	-75.36440	-75.36440
H ₂ O	-75.99343	-75.99205	-75.99439
CH ₃ CHO	-152.84801		-152.84810

4-31+G in both reactions. Finally, that the 6-31++G are, in both cases, approximations from below to the experimental ones, while the 4-31G results are approximations from above also in both situations. Consequently, we may think that, although not exact, the use of 6-31++G and 4-31G may provide a kind of bracketing technique to estimate the correct energies for proton transfers in gas phase.

A final point concerns geometry optimizations. 6-31++G optimized geometries did not afford any major modification of the energies, as can be seen in Table

3. Making the exception of H₂O (and H₃O⁺, too) we see that it is reasonable to use 4-31G optimized geometries in 6-31++G calculations as we did in the rest of the paper (6-31G* optimized geometries were used for water and H₃O⁺ for the reasons given above). Geometry optimizations were done using Schlegel's algorithm [16] as coded in the GAUSSIAN80 package [17], or by minimization of the norm of the gradient [18] using the VA05 option of the MONSTERGAUSS system of programs [19]. SCF calculations and optimizations were done at the IBM 3031 of the CNUCE, Pisa, Italy and the Burroughs 6930 of Di.C.U.R., Montevideo, Uruguay.

3.2. Solvation method

Bulk solvent effects were modelled using the continuum solvation method of Ref. [20] coded into the GAUSS70 program [21]. In this model the solute is represented by its charge distribution $\rho(\mathbf{r})$ in a cavity embedded into an infinite polarizable dielectric medium with permittivity ϵ (which we shall take equal to 80.0 to simulate water throughout this work).

In practice, the polarization of the dielectric due to the solute is reduced to the creation of a system of virtual charges on the cavity surface, with density $\sigma(\mathbf{s})$ (different from zero only at this surface, a fact indicated by using vector \mathbf{s} in place of \mathbf{r}). This surface charge distribution produces an electrostatic potential, $V_\sigma(\mathbf{r})$, which is added to the solute hamiltonian H^0 to account for the polarization produced by the solvent in this model

$$H = H^0 + V_\sigma.$$

To generate the charge distribution $\sigma(\mathbf{s})$, the surface of the cavity, S , is divided into portions ΔS small enough to consider $\sigma(\mathbf{s})$ constant on each of them. This constancy is tested through the convergence of different properties with the increase of the number of those area elements, as may be seen in Table I of [22]. The cavity is built as a system of interlocked spheres, centered on each nucleus of the solute, with radii R_k (chosen to be 1.20 times the van der Waals radii of the atoms, due to reasons already discussed in [22]). Each portion of S , corresponding to the k -th sphere, is further partitioned in the aforementioned portions ΔS_{ki} . The area of each element is calculated and $\sigma(\mathbf{s})$ evaluated at the center of each element using the basic relation

$$\sigma(\mathbf{s}) = -[(\epsilon - 1)/4\pi\epsilon]E(\mathbf{s})_{n^-},$$

where $E(\mathbf{s})_{n^-}$ is the electric field evaluated in vacuum (i.e., inside the cavity [20]). However, $E(\mathbf{s})_{n^-}$ depends on $\sigma(\mathbf{s})$ and, consequently, an iterative process is necessary. Once this process has converged, the final charges obtained at each element through the density $\sigma(\mathbf{s}_{ki})$

$$q_{ki}^{of} = \sigma^{of}(\mathbf{s}_{ki})\Delta S_{ki}$$

are used to create the potential V_σ which is utilized, in turn, to polarize the initial charge distribution of the solute, $\rho^0(\mathbf{r})$. A safeguard is installed to prevent two charges being too close, avoiding thus possible divergences as would be the case

in other contexts [23] (the results are not affected by the presence of this control mechanism). The process is iterated self-consistently until a converged solute density $\rho^f(\mathbf{r})$ and system of charges q_{ki}^f is obtained (thus, two types of SCF cycles are necessary, one to obtain the potential V_σ and the other to solve the Hartree-Fock equations with the modified potential within each cycle of the former type).

The difference between the energies obtained with and without the continuum model of the solvent will be denoted in this work as ΔG_{el} , and will be said to measure the electrostatic contribution to the solvation energy. Although we are not directly interested in the problem of accurate estimates of the standard free energy of solvation, ΔG_h° , because all the processes considered in this paper regard species in solution and there is a noticeable compensation among ΔG_h° for different solutes, a brief sketch of the relation between ΔG_h° and ΔG_{el} may clarify the virtues and shortcomings of the method. To this end, we shall use a relatively crude model, able to give an *ab initio* appreciation of ΔG_h° , where ΔG_{el} will find its appropriate place. We emphasize that in the following calculations we did not introduce any *ad hoc* calibration factor and reduced to a minimum the use of empirical parameters.

The transfer process may be schematized in two steps: the formation of a mol of cavities of suitable size, and the insertion of the molecules of the solute M into them

$$\Delta G_h^\circ = G_{cav} + \Delta G_{sol}.$$

The cavitation free energy, G_{cav} , will be computed with Pierotti's formula [24]. For cavities of the size considered in this paper, the numerical values are not very different from Sinanoglu's estimates [25]. The second term is the difference in free energy of two systems composed by (a) the solvent S' with the cavities plus the gaseous solute M , and (b) the dilute solution. Standard states are ideal gas at $P = 1$ atm and the hypothetical solution at unit molarity (without solute-solute interactions). Making the additional hypothesis that the effect of the insertion of M in S' is limited to the polarization of the solvent, of which account will be taken in the definition of the reference energies, we may write

$$\Delta G_{sol} = G_{(M \text{ in sol})} - G_{(M \text{ gas})}$$

and

$$\Delta G_{sol} = \Delta(PV) - RT \ln(Q_{sol}^M / Q_{gas}^M),$$

where Q^M is the molecular partition function of the solute.

It is convenient to collect the terms of this last equation in the following way, dropping the index M for simplicity

$$\Delta G_{sol} = -RT - RT \ln[(V_{sol}/V_{gas})(Q_{sol}^{vib}/Q_{gas}^{vib})(Q_{sol}^{lib}/Q_{gas}^{rot})] - \Delta E^{eff}$$

with the obvious meaning of therms. Each one of them deserves a detailed discussion, which will be limited here to a few remarks.

3.2.1. Translational contribution

It is affected by the choice of the reference state and by some problems of principle (communal entropy, entropy of liberation). Of particular importance is the definition of V_{sol} , for which we adopted the ideas of the cell model. V_{sol} is thus the “free volume” [26] or the “fluctuation volume” [27]. We employed values derived from partial molar volumes and van der Waals areas and volumes. Other estimates (e.g. from sound velocity) gave similar results.

3.2.2. Vibrational contributions

Zero point energies are collected here, because our partition functions are measured from the bottom of the potential well. The contribution of this term is, in general, modest except for some low frequency motions or for stretching modes for H atoms involved in hydrogen bonds with the solvent. We adopted the approximation of non-interacting modes, computed energy curves for the interesting low frequency motions *in vacuo* as well as in solution, and introduced first order corrections to the X-H stretching contributions on the basis of the results of a dimeric X-H·H₂O model.

3.2.3. Rotational-librational contributions

Rotational contributions were obtained from our geometries *in vacuo*. Librational contributions have been estimated by allowing independent librational motions of M in a supermolecular cluster mimicking the first solvation shell (only STO-3G calculations; the almost perfect coincidence with the value of this term for H₂O in water drawn from experimental data is surely due to numerical accident).

3.2.4. ΔE^{eff}

It may be interpreted as a free energy change and written as

$$\Delta E^{\text{eff}} = E_{\text{sol}} - E_{\text{gas}}.$$

For the solute in gaseous state internal energy and free energy coincides (at $T = 0^\circ\text{K}$). The energy of M , including the interaction with the polarized solvent, E_{sol} , has the status of a free energy. It may be divided into

$$E_{\text{sol}} = E_{\text{el}} + E_{\text{dis}}.$$

Repulsive solute-solvent terms are accounted for by G_{cav} . For the dispersion term we have employed a perturbation-like formula similar to that used in [28] for dispersion-repulsion contributions. The numerical results have been compared with those obtained with Claverie’s method [29]; a better agreement is obtained with 4-31G than with the STO-3G basis set. The electrostatic term E_{el} will be given as the energy obtained with $\epsilon = 80.0$ in the following. It may also be written more explicitly in terms of the expectation value of the solvent modified hamiltonian of M , H , and the work spent to polarize the dielectric, $\frac{1}{2}\langle\psi'|V_\sigma|\psi'\rangle$, as

$$E_{\text{el}} = \langle\psi'|H|\psi'\rangle - \frac{1}{2}\langle\psi'|V_\sigma|\psi'\rangle,$$

with V_σ the reaction potential as described previously. For further details on the derivation of this equation see [20, 30–31]. Finally, ΔG_{el} is defined as

$$\Delta G_{el} = E_{el} - E_{gas}$$

and as such will be used in the following.

We report in Table 4 a specimen of results obtainable with these approximations. The results obtained with the STO-3G and 4-31G basis sets seem to bracket the experimental value (the “experimental” estimate for $\text{CH}_2=\text{CHOH}$ is but a simple guess). ΔG_{el} values, as employed in the text, emphasize the stability of the solution; differences with respect to $\Delta G_h^\circ(\text{exp})$ values are, however, confined within reasonable limits.

In all the calculations done in this paper we used approximation IV of [20]. The number of points used to divide each atomic sphere into ΔS_{ki} elements was 326, corresponding to increments of 18° in each angle over the surface of the sphere. As shown in Table III and Figs. 2–4 of [20], this choice is a good one, since both energy and dipole moment have converged to their limit values. Mutual polarization of charges composing $\sigma(s)$ was allowed until convergence in each SCF cycle, and iteration of all the calculations were done until the energy of interaction was not modified in more than 10^{-5} a.u.. Different orientation of the local axis and then different definitions of the area elements ΔS_{ki} produce only small changes in ΔG_{el} (less than 0.05 kcal/mol). Some numerical values evidencing the low dependence of ΔG_{el} on the selection of the area elements and on the intersection of the spheres are reported in a forthcoming paper [43].

All calculations of solvent effects were done with the GOULD-SEL minicomputer of the Institute of Quantum Chemistry and Molecular Energies of the C.N.R., Pisa, Italy.

Table 4. Estimates of ΔG_h° in kcal/mol

	H_2O		CH_3CHO		CH_2CHOH	
	STO-3G	4-31G	STO-3G	4-31G	STO-3G	4-31G
G_{cav}	5.19	5.19	9.20	9.20	9.00	9.00
$-RT$	-0.59	-0.59	-0.59	-0.59	-0.59	-0.59
$-RT \ln \frac{V(\text{sol})}{V(\text{gas})}$	6.78	6.78	6.64	6.64	5.57	5.57
$-RT \ln \frac{Q_{vib}(\text{sol})}{Q_{vib}(\text{gas})}$	-0.73	-0.66	-0.30	-0.20	-0.55	-0.40
$-RT \ln \frac{Q_{iib}(\text{sol})}{Q_{rot}(\text{gas})}$	1.14	(1.14) ^d	2.44	(2.44) ^d	2.54	(2.54) ^d
ΔG_{el}	-4.09	-8.84	-3.07	-8.94	-3.42	-6.81
G_{disp}	-7.40	-7.29	-10.59	-9.90	-10.10	-9.05
$\Delta G_h^\circ(\text{calc})$	0.29	-4.28	3.37	-1.35	2.45	0.46
$\Delta G_h^\circ(\text{exp})$		-1.98 ^a		0.77 ^b		-1.44 ^c

^a Calculated from data in [32]

^b [33] as quoted in [34]

^c STO-3G values assumed

^d Estimated on the basis of additive group contributions [34]

4. Results and discussion

4.1. Concerted water-chain mechanism in gas phase

Capon et al. [7] suggested the possibility that a concerted mechanism was acting in place of reactions (1) and (2). That is, one water molecule would be abstracting the hydroxilic proton from vinyl alcohol while another one is donating a proton to the CH_2 group. We studied in [1a] the feasibility of such a mechanism where both proton-donating and proton-abstracting water molecules were part of a dimer interacting with vinyl alcohol. We found this mechanism to be much more favorable for the reaction in gas phase than the simple 1,3-proton migration. A similar behavior was reported by Williams and Maggiora on the assistance of a second H_2O molecule to the addition of water to formaldehyde [35] and by ourselves on the reaction of HF and HCl dimers with ethylene [36].

Since the calculations in [1a] were done using the semiempirical CNDO/2 method and the *ab initio* one with the minimal STO-3G basis set we thought that an improvement of the level of calculation was necessary to compare that mechanism with the ones of reactions (1), (2) and (3), (4) respectively. Therefore, we optimize the geometry of the structures corresponding to the critical points on the hypersurface for this mechanism using the 4-31G basis set. No calculations are reported using the 6-31++G basis set at the 4-31G optimized structures for two reasons. First, severe convergence problems were found in the SCF process at both transition points structures TS1 and TS2. Second, the calculation of the energy difference between vinyl alcohol and acetaldehyde at the 4-31G//4-31G level ($\Delta E = -9.9$ kcal/mol) and at the 6-31++G//4-31G level ($\Delta E = -8.2$ kcal/mol) showed little difference, suggesting that not a very large improvement should be expected through this amelioration of the basis set.

The geometric parameters of those structures at the 4-31G level and at the STO-3G one (taken from [1a]) are given in Table 5 together with the optimized geometries of the other species discussed in this paper. The overall appearance of the complexes is not very different from that in the figures of [1a]. Hence they are not reproduced here. The 4-31G optimized geometry of the transition state for the 1,3-proton migration at the 4-31G level is coincident with the one given previously by Rodwell et al. [37].

The energetic facet of the calculations is collected in Table 6. Two main effects are seen when passing from STO-3G to 4-31G. First, the barrier ΔE_2 is increased in 4-31G with respect to STO-3G, due mainly to destabilization of TS2. Second, there is almost the same difference in energy between the water complexes of acetaldehyde and vinyl alcohol than between the isolated molecules when 4-31G is used. This differs neatly from the STO-3G result and is in agreement with the hydrogen bonding ability of the $\text{C}=\text{COH}$ and $\text{C}-\text{CH}=\text{O}$ structures. The differences between ΔE_{-2} and ΔE_{-1} are smaller in 4-31G (46.6 and 47.8 kcal/mol respectively) than in STO-3G calculations (69.9 and 74.8 kcal/mol respectively). However, they are still large enough to make our assertion on the preeminence of hydrated-cluster water chain mechanism over 1,3-proton migration in gas phase [1a] still valid. However, the large value of ΔE_2 in 4-31G casts some doubt

Table 5. Optimized structures of the species intervening in this work (distances are in Å, angles in degrees)

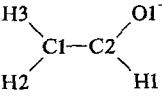
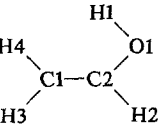
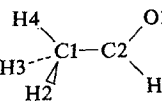
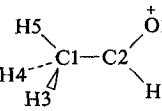
Species ^a	Point Group	Parameter	STO-3G	4-31G	6-31++G	Experiment
HO ⁻	<i>C_{∞v}</i>	O-H	1.068	0.984	0.965	0.989 ^b
H ₂ O	<i>C_{2v}</i>	O-H	0.989	0.950	0.950	0.958 ^c
		<HOH	100.0	111.2	112.6	104.5 ^c
H ₃ O ⁺	<i>D_{3h}, C_{3v}</i>	O-H	0.990	0.964	0.964	
		<HOH	113.8	120.0	117.7	111.3 ^d
	<i>C_s</i>	C1-C2	1.372	1.357		
		C2-O1	1.269	1.280		
		C2-H1	1.124	1.107		
		C1-H2	1.073	1.077		
		C1-H3	1.073	1.077		
		<C1C2O1	131.4	130.7		
		<C1C2H1	111.4	113.2		
		<C2C1H2	121.4	121.0		
		<C2C1H3	122.4	121.3		
	<i>C_s</i>	C1-C2	1.312	1.315	1.332 ^e	
		C2-O1	1.390	1.371	1.373 ^e	
		O1-H1	0.989	0.952	0.956 ^e	
		C2-H2	1.089	1.068	1.079 ^e	
		C1-H3	1.077	1.069	1.078 ^e	
		C1-H4	1.080	1.073	1.090 ^e	
		<C1C2O1	126.7	126.5	126.0 ^e	
		<C2O1H1	105.2	115.0	108.5 ^e	
		<C1C2H2	122.2	123.5	123.7 ^e	
		<C2C1H3	121.2	120.5	119.5 ^e	
		<C2C1H4	122.0	122.6	121 ^e	
	<i>C_s</i>	C1-C2	1.536	1.494	1.494	1.501 ^e
		C2-O1	1.217	1.209	1.215	1.216 ^e
		C2-H1	1.104	1.085	1.085	1.114 ^e
		C1-H2	1.087	1.084	1.085	
		C1-H3	1.087	1.084	1.085	
		C1-H4	1.085	1.079	1.081	
		<C1C2O1	124.3	124.2	124.0	123.9 ^e
		<C1C2H1	114.3	116.0	116.7	117.5 ^e
		<C2C1H2	109.9	110.2	110.4	
		<C2C1H3	109.9	110.2	110.4	
		<C2C1H4	110.5	110.3	110.0	
		<O1C2C1H2	120.6	120.9	120.9	
	<i>C_s</i>	C1-C2	1.516	1.457		
		C2-O1	1.281	1.261		
		O1-H1	0.999	0.963		
		C2-H2	1.113	1.077		
		C1-H3	1.093	1.088		
		C1-H4	1.093	1.088		
		C1-H5	1.089	1.077		
		<C1C2O1	119.3	119.8		
		<C2O1H1	114.0	123.3		

Table 5 (continued)

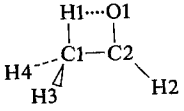
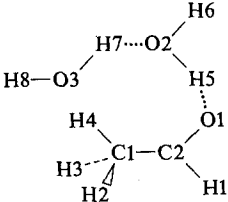
Species ^a	Point group	Parameter	STO-3G	4-31G	Experi- ment
		<C1C2H2	120.7	121.3	
		<C2C1H3	108.1	109.2	
		<C2C1H5	109.9	111.8	
		<O1C2C1H3	120.6	122.3	
	C_s	C1-C2	1.447	1.367	
		C2-H2	1.097	1.080	
		C2-O1	1.292	1.362	
		O1-H1	1.475	1.511	
		C1-H3	1.087	1.072	
		C1-H4	1.082	1.071	
		<O1C2C1	102.6	124.3	
		<H2C2C1	136.5	116.5	
		<H1C1C2	67.2	44.6	
		<H3C1C2	108.0	119.3	
		<H4C1C2	118.9	120.9	
		<H1O1C2C1	3.3	1.2	
		<H3C1C2O1	151.7	176.1	
		<H4C1C2O1	-81.7	-62.2	
		<H2C2C1O1	183.0	181.7	
	C_s	C1-C2	1.534	1.487	
		C2-O1	1.220	1.218	
		H1-C2	1.105	1.083	
		H4-C1	1.085	1.079	
		H3-C1	1.087	1.082	
		H2-C1	1.087	1.084	
		H5-O1	1.850	1.878	
		O2-H5	0.985	0.958	
		H6-O2	0.985	0.948	
		H7-O2	1.749	1.805	
		O3-H7	0.989	0.962	
		H8-O3	0.988	0.949	
		<O1C2C1	124.3	124.4	
		<H1C2C1	114.8	116.5	
		<H4C1C2	110.4	110.4	
		<H3C1C2	109.5	108.9	
		<O1C2C1	128.3	127.4	
		<H2C2C1	119.9	121.7	
		<H3C1C2	122.3	120.2	
		<H4C1C2	121.0	122.3	
		<H1O1C2	107.4	116.3	
		<O2H1O1	177.7	165.9	
		<H5O2H1	111.8	120.2	
		<H6O2H1	111.6	106.3	
		<O3H6O2	177.5	163.7	
<H8O3H6	111.5	104.8			
<H7O3H6	113.2	126.2			
<H2C2C1O1	180.0	180.0			
<H3C1C2O1	180.0	180.0			
<H4C1C2O1	0.0	0.0			

Table 5 (continued)

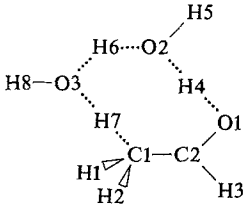
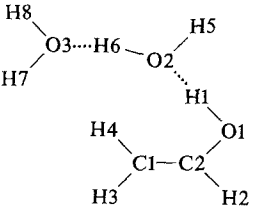
Species ^a	Point group	Parameter	STO-3G	4-31G	Experi- ment
	<i>C_s</i>	<O2H1O1C2	51.6	45.6	
		<H5O2H1O1	125.0	127.1	
		<H6O2H1O1	10.8	-2.5	
		<O3H6O2H1	27.0	10.9	
		<H7O3H6O2	-31.4	-26.2	
		<H8O3H6O2	-145.1	-159.1	
		<H1O1C2C1	2.2	11.2	
		C1-C2	1.416	1.398	
		C2-O1	1.279	1.276	
		C2-H3	1.104	1.092	
		H4-O1	1.204	1.279	
		O2-H4	1.127	1.104	
		H5-O2	0.980	0.960	
		H6-O2	1.129	1.166	
		<H2C1C2	109.9	110.1	
		<H5O1C2	120.2	120.1	
		<O2H5O1	165.6	160.0	
		<H6O2H5	102.6	113.2	
		<H7O2H5	106.1	99.7	
		<O3H7O2	167.2	162.9	
		<H8O3H7	100.8	111.7	
		<H1C2C1O1	180.3	179.0	
		<H4C1C2O1	-3.5	-4.0	
		<H3C1C2O1	116.2	115.1	
		<H2C1C2O1	-124.6	-125.5	
		<H5O1C2H1	122.4	120.5	
<O2H5O1C2	-0.9	-5.0			
<H6O2H5O1	174.2	167.5			
<H7O2H5O1	0.0	-6.5			
<O3H7O2H5	-6.4	-16.3			
<H8O3H7O2	-134.7	-132.0			
	<i>C_s</i>	C1-C2	1.317	1.323	
		C2-O1	1.371	1.353	
		C2-H2	1.091	1.070	
		H1-O1	1.005	0.968	
		O2-H1	1.541	1.779	
		H5-O2	0.983	0.963	
		O3-H6	1.618	1.794	
		H7-O3	0.986	0.954	
		H8-O3	0.986	0.950	
		H3-C1	1.077	1.072	
		H4-C1	1.076	1.071	
		<O1C2C1	128.3	127.4	
		<H2C2C1	119.9	121.7	
		<H3C1C2	122.3	122.3	
		<H4C1C2	121.0	120.2	
		<H1O1C2	107.4	116.3	
		<O2H1O1	177.7	165.9	
		<H5O2H1	111.8	120.2	

Table 5 (continued)

Species ^a	Point group	Parameter	STO-3G	4-31G	Experi- ment
		<H6O2H1	111.6	106.3	
		<O3H6O2	177.5	163.7	
		<H8O3H6	111.5	104.8	
		<H7O3H6	113.2	126.2	
		<H2C2C1O1	180.0	180.0	
		<H1O1C2C1	2.2	11.2	
		<H3C1C2O1	180.0	180.0	
		<H4C1C2O1	0.0	0.0	
		<O2H1O1C2	51.6	45.6	
		<H5O2H1O1	125.0	127.1	
		<H6O2H1O1	10.8	-2.5	
		<O3H6O2H1	27.0	10.9	
		<H7O3H6O2	-31.4	-26.2	
		<H8O3H6O2	-145.1	-159.1	

^a The structures were schematized in order to clarify the numbering of the atoms

^b [38]

^c [39]

^d [40]

^e [41], [42]

Table 6. Relative energies of the species involved in the gas-phase 1,3-proton migration and hydrated-cluster water-chain mechanisms for the conversion of vinyl alcohol to acetaldehyde, and barriers for the reactions (in kcal/mol)

Energy differences ^a	STO-3G//STO-3G	4-31G//4-31G
$\Delta E_0(\text{CH}_2\text{CHOH} + 2\text{H}_2\text{O})$	0.0	0.0
$\Delta E_0(\text{TS1}^b + 2\text{H}_2\text{O}) = \Delta E_1$	91.7	82.4
$\Delta E_0(\text{CH}_3\text{CHO} + 2\text{H}_2\text{O})$	-18.4	-9.9
ΔE_{-1}	110.1	92.8
$\Delta E_0(\text{CH}_2\text{CHOH} \cdot (\text{H}_2\text{O})_2)$	-17.8	-20.4
$\Delta E_0(\text{TS2}^c)$	4.0	15.4
$\Delta E_0(\text{CH}_3\text{CHO} \cdot (\text{H}_2\text{O})_2)$	-31.3	-29.6
ΔE_2	21.8	35.8
ΔE_{-2}	35.3	45.0

^a ΔE_0 is the relative energy with respect to vinyl alcohol plus two water molecules infinitely apart (STO-3G = -300.84848 a.u., 4-31G = -304.48802 a.u., see Table 7). ΔE_1 is the barrier for the transformation of vinyl alcohol in acetaldehyde through the 1,3-proton migration mechanism. ΔE_{-1} is the barrier for the transformation of acetaldehyde to vinyl alcohol through the 1,3-proton migration mechanism. ΔE_2 is the same as ΔE_1 but through the hydrated-cluster water-chain mechanism. ΔE_{-2} is the same as ΔE_{-1} but through the hydrated-cluster water-chain mechanism

^b TS1 is the symbol for the 1,3-proton migration transition state

^c TS2 is the symbol for the hydrated-cluster water-chain mechanism transition state

about the feasibility of such a mechanism. More detailed and careful theoretical study of this system, coupled with experiments using hydrated clusters in gas phase or in aprotic solvents without hydrogen bonding ability are needed to settle the matter and are under way.

4.2. Comparison with other mechanisms in gas phase and in solution

In Table 7 are collected the total energies of the species reported as yet and in the following, using the optimized geometries of Table 5. With these energies we have drawn the schemes of Figs. 1 and 2, where the four mechanisms (i.e. 1,3-proton migration, water-chain, Capon's one and that of reactions (3) and (4)) are compared in gas phase and in aqueous solution respectively. The energy of TS1 has been included in Fig. 1 only since it is hardly probable that it is present in protic solvents.

In Fig. 1 the features already mentioned with respect to the water-chain mechanism and 1,3-proton migration may be seen clearly. Also shown are the energies corresponding to the intermediate steps in reactions (1), (2) and (3), (4). As expected, the participation of ions will not be important, not even probable, in gas phase. However, it is very instructive to observe the difference in energy between $\text{CH}_3\text{CHOH}^+ + \text{HO}^-$ and $\text{CH}_2\text{CHO}^- + \text{H}_3\text{O}^+$. According to the experimental values of the proton affinities reported in Table 1, the difference should give something between -5.5 and -3.1 kcal/mol. The values given by the STO-3G, 4-31G and 6-31++G basis sets are respectively 54.5, 23.2 and -1.1 kcal/mol showing that the former two sets are even qualitatively wrong whilst the latter one is fairly satisfactory. On the other side, for neutral molecules both 4-31G and 6-31++G are very similar, as is demonstrated by the energy difference between both isomers (-9.9 and -9.2 kcal/mol respectively) which agrees well with the experimental pK_{enoi} of 6.66 and 6.44 found by Capon et al. [7].

In Fig. 2 are shown the results obtained when the solvent field is applied. As to the general appearance of the scheme it is seen that the relative energies of the ionic intermediates are lowered whilst those of the water complexes and the TS2 transition state are increased with respect to their values in gas phase. This behavior is not unexpected for two reasons. On one side, the ionic species induce opposite charges in the dielectric which simulates bulk solvent. Through mutual polarization of the dielectric and solute's charge distributions an equilibrium is reached where the high energy needed to create the ions is diminished by smearing out the charge of the solute by the "solvent". On the other side, for the neutral water complexes and the transition state the relative energies increase due to the fact that part of the solvation energy recovered by the continuum model is lost when water is hydrogen-bounded to acetaldehyde or vinyl alcohol in place of being as free molecules (see the section on the definition of ΔG_{el}).

The barrier for the transformation of vinyl alcohol to acetaldehyde through the water-chain mechanism is not noticeably modified by the inclusion of the solvent field: it is increased by about 3 kcal/mol, most probably an artifact of the method. Comparing this value (38.5 kcal/mol) with those of the ionic intermediates given

Table 7. Total energies (in a.u.) of the species considered in this work. Gas phase ($\epsilon = 1$) and solution ($\epsilon = 80$) results

Species	$\epsilon = 80.0^a$					
	STO-3G//STO-3G	4-31G//4-31G	6-31++G//4-31G	STO-3G//STO-3G	4-31G//4-31G	6-31++G//4-31G
HO ⁻	-74.06502	-75.22979	-75.36440	-74.20834	-75.38530	-75.51362
H ₂ O	-74.96590	-75.90864	-75.99205 ^b	-74.97241	-75.92273	-76.00771 ^b
H ₃ O ⁺	-75.33044	-76.20060	-76.27092 ^b	-75.46439	-76.33296	-76.40928 ^b
CH ₂ CHO ⁻	-150.14445	-152.06245	-152.24959	-150.25564	-152.18194	-152.36770
CH ₂ CHOH	-150.91668	-152.67074	-152.83332	-150.92137	-152.68159	-152.84646
CH ₃ CHO	-150.94599	-152.68652	-152.84801	-150.95082	-152.70076	-152.86218
CH ₃ CHOH ⁺	-151.32310	-152.99628	-153.15440	-151.43268	-153.10821	-153.26545
CH ₂ CHOH·(H ₂ O) ₂	-300.87685	-304.52047		-300.89186	-304.55011	
CH ₃ CHO·(H ₂ O) ₂	-300.89836	-304.53517		-300.90990	-304.56164	
TS1 ^c	-150.77052	-152.53860				
TS2 ^c	-300.84211	-304.46340		-300.85310	-304.48872	

^a ϵ is the dielectric constant of the medium^b 6-31G* geometries used, see text^c TS1 and TS2 as defined in Table 5

Fig. 1. Gas-phase energies of the different species considered in this work (in kcal/mol). The energy of one or two water molecules was added when necessary to keep all mechanisms in the same scheme and, when so done is shown in the label of each energy. TS1 stands for the transition state of the 1,3-proton migration mechanism, TS2 for the transition state of the water-chain mechanism, EW2 and KW2 are the complexes of vinyl alcohol and acetaldehyde, respectively, with two water molecules. Continuous lines, broken lines and alternated points and lines are STO-3G, 4-31G and 6-31++G energies, respectively

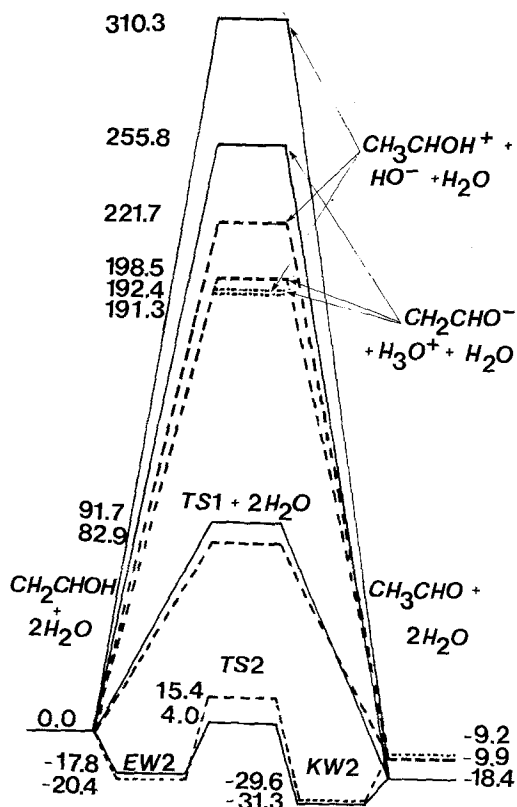


Fig. 2. Same as Fig. 1 but in solution ($\epsilon = 80.0$). The energies of TS1 with different basis sets is not shown, as said in the text

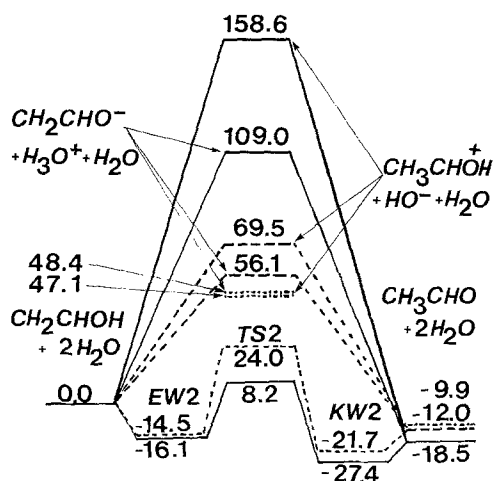


Table 8. Relative energies (in kcal/mol) with respect to vinyl alcohol and HO⁻ of the species in reactions (5), in gas phase and in solution

Species	STO-3G//STO-3G		4-31G//4-31G		6-31++G//4-31G	
	$\epsilon = 1.0$	$\epsilon = 80.0$	$\epsilon = 1.0$	$\epsilon = 80.0$	$\epsilon = 1.0$	$\epsilon = 80.0$
CH ₂ CHOH+HO ⁻	0.0	0.0	0.0	0.0	0.0	0.0
CH ₂ CHO ⁻ +H ₂ O	-80.7	-61.7	-44.3	-23.7	-27.6	-9.6
CH ₃ CHO+HO ⁻	-18.4	-18.5	-9.9	-12.0	-9.2	-9.9

Table 9. Relative energies (in kcal/mol) with respect to vinyl alcohol and H₃O⁺ of the species in reactions (6), in gas phase and in solution

Species	STO-3G//STO-3G		4-31G//4-31G		6-31++G//4-31G	
	$\epsilon = 1.0$	$\epsilon = 80.0$	$\epsilon = 1.0$	$\epsilon = 80.0$	$\epsilon = 1.0$	$\epsilon = 80.0$
CH ₂ CHOH+H ₃ O ⁺	0.0	0.0	0.0	0.0	0.0	0.0
CH ₂ CHOH ⁺ +H ₂ O	-26.3	-12.1	-21.1	-10.3	-26.5	-10.9
CH ₃ CHO+H ₃ O ⁺	-18.4	-18.5	-9.9	-12.0	-9.2	-9.9

by the 6-31++G basis set (which is not a wrong comparison taking into account what has been said up to now concerning the effect of basis sets), 48.4 and 47.1 kcal/mol, we see that, within the approximate nature of the methods we are using, it may be that the three mechanisms are equally probable (especially taking into account that the barrier for the water-chain mechanism should be increased if the components of ΔG for complexation were taken into account). Therefore, it seems that, contrary to the case in gas phase, there is no definite reason to prefer the water-chain mechanism over Capon's one or that of reactions (3) and (4) in water solution. It is conceivable that the three of them are occurring at more or less the same rate and equally contributing to the overall reaction.

4.3. Acid and base catalysis

According with Capton et al. [7] the enolization of vinyl alcohol can be general acid or base catalyzed. These processes correspond to reactions (5) and (6) respectively and we studied their thermodynamical aspects in Tables 8 and 9.

With respect to base catalysis we see that in gas phase it is fairly easy for HO⁻ to abstract a proton from the hydroxyl group of vinyl alcohol, keeping it to form water. On the contrary, it will be difficult for enolate anion to do the same to water. However, in solution this is an allowed process and water can donate a proton to the CH₂ end of enolate to form acetaldehyde and again the hydroxide ion. This donation is predicted only by 6-31++G calculations which show the correct tendency as we said before.

The opposite situation is observed with respect to acid catalysis. Although in gas phase all basis sets confirm the unfeasibility of water protonation by CH₃CHOH⁺, both STO-3G and 4-31G allowed it in solution. However, the more correct

6-31++G results show that it is necessary a small energy waste for water to abstract a proton from the oxygen atom of CH_3CHOH^+ .

These facts are in qualitative agreement with the experimental finding that base catalysis is favored over acid one [7]. However, the small differences found between both mechanisms are not in quantitative agreement with the large difference between k_{H^+} and k_{HO^-} . An explanation of this fact may perhaps be found in the kinetic details of the attack of both H_3O^+ and HO^- .

To see whether any barrier for the transference of a proton is found in gas phase, we performed geometry optimizations of the complexes $\text{HO}^- \cdot \text{CH}_3\text{CHO}$, $\text{H}_3\text{O}^+ \cdot \text{CH}_2\text{CHO}^-$ and $\text{CH}_2\text{CHO}^- \cdot \text{H}_3\text{O}^+$ at the STO-3G level. The most important parameters of the optimized complexes are shown in Fig. 3. In the first case, which mimic the attack of HO^- on the methyl group of acetaldehyde, the final product was a hydrogen-bonded complex of the type found by Chaillet et al. [44], with an optimum intermolecular distance of 1.548 Å. The stabilization energy of this complex with respect to vinyl alcohol and HO^- is 100.6 kcal/mol, 19.6 kcal/mol more stable than enolate plus water (obviously, these figures are heavily influenced by basis set superposition error [45]). No gas phase barrier was detected. Instead, the proton was transferred in the course of the optimization. Completely similar results were found for the other two complexes, obtaining $\text{H}_2\text{O} \cdot \text{CH}_3\text{CHO}$ and $\text{CH}_2\text{CHOH} \cdot \text{H}_2\text{O}$ respectively. Therefore, the conclusion to arrive is that whatever barrier may be present in solution should be ascribed to solvent reorganization and diffusion processes since no intrinsic barrier is found in gas phase.

In conclusion, although no geometry optimizations could be done including the

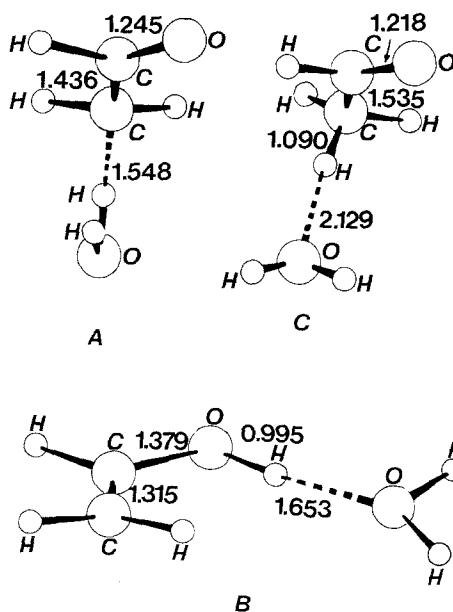


Fig. 3. Geometrical structures, showing the values of the most important parameters, obtained with the STO-3G basis set for the attack of HO^- to CH_3CHO , (A), and H_3O^+ to CH_2CHO^- at oxygen, (B), and carbon, (C), respectively (lengths shown are in Å)

solvent field, it seems that the main differences which are present experimentally between acid and base catalysis emerge from desolvation/diffusion barriers, which were not studied in this work, and from the thermodynamic stability of the products with respect to the intermediates.

5. Conclusions

According to the results shown in this paper, ketonization of vinyl alcohol in gas phase is greatly speeded up by the action of water molecules through a water-chain mechanism. The barrier for the transformation is decreased by almost 50 kcal/mol at the 4-31G level. However, it still remains sufficiently high as to allow vinyl alcohol to be present in gas phase quite a long time (although the simultaneous transference of protons between two vinyl-alcohol molecules was not studied in this work, we believe this mechanism is not going to alter this conclusion).

Ionic mechanisms are completely unfavorable in gas phase, as expected. The necessity of employing better basis sets than STO-3G or 4-31G to study the ionic mechanisms is concluded from the comparison with 6-31++G data.

Using the continuum method of solvation a large part of the solvation energy is recovered. In particular, it was shown that mechanisms involving ionic intermediates should be as important as the water-chain one in solution.

With respect to acid and base catalysis it is noted that whilst the latter one implies a facile conversion of vinyl alcohol to acetaldehyde, the former one needs to surmount a small barrier to perform the conversion. The order of importance of these processes in neutral water solutions found experimentally: base catalysis more important than acid catalysis more important than water catalysis is reflected qualitatively in the barriers to be overcome in each process. However, the methods employed do not allow us to obtain quantitative agreement with experiment.

With respect to the methods employed we conclude that diffuse functions are needed to produce qualitatively correct gas phase results. In solution, the continuum method allows the recovery of a large part of the solvation energy. However, further improvements in basis sets and solvation methods are needed to fully address the problem studied in this paper.

Acknowledgements. O.N.V. acknowledges the receipt of a grant from The Rotary Foundation of Rotary International to work at the laboratories in Spain and Italy where part of this work was done. UNPD support under project URU/84/002 PEDECIBA is also acknowledged.

References and notes

- (a) Lledós A, Bertrán J, Ventura ON *Int J Quantum Chem*, in press;
(b) Lledós A, Bertrán J (1981) *Tetrahedron Lett* 775;
(c) Bertrán J, Lledós A, Revellat JA (1983) *Int J Quantum Chem* 23:587;
(d) Lledós A, Bertrán J (1984) *J Mol Struct* 107:233;
(e) Lledós A, Bertrán J (1985) *J Mol Struct* 120:73
- Ventura ON, Bartolucci JP (1984) *Theor Chim Acta* 64:229 and references therein
- (a) Muñiz MA, Bertrán J, Andrés JL, Durán M, Lledós A (1985) *J Chem Soc Faraday Trans 1* 81:1547;
(b) Newton MD (1977) *J Chem Phys* 67:5535

4. (a) Toullec J (1982) *Adv Phys Org Chem* 18:1;
(b) Hart H (1979) *Chem Rev* 79:515
5. Saito S (1976) *Chem Phys Lett* 42:399
6. (a) Blank B, Fischer H (1973) *Helv Chim Acta* 56:506;
(b) Blank B, Henne A, Laroff GP, Fischer H (1975) *Pure Appl Chem* 41:475
7. (a) Capon B, Rycroft DS, Watson TW, Zucco C (1981) *J Am Chem Soc* 103:1761;
(b) Capon B, Zucco C (1982) *J Am Chem Soc* 104:7567
8. (a) Guthrie JP, Cullimore PA (1979) *Can J Chem*;
(b) Guthrie JP (1979) *Can J Chem* 57:797;
(c) Guthrie JP (1979) *Can J Chem* 57:1177
9. Hehre WJ, Stewart RF, Pople JA (1969) *J Chem Phys* 51:2657
10. Ditchfield R, Hehre WJ, Pople JA (1971) *J Chem Phys* 54:724
11. Radom L (1977) *Mod Theor Chem* 4:333
12. Chandrasekhar J, Andrade JG, Ragué-Schleyer PV (1981) *J Am Chem Soc* 103:5609 and references therein
13. Cao HZ, Tapia O, Evleth EM (1985) *J Phys Chem* 89:1581
14. (a) Krishnan R, Binkley JS, Seeger R, Pople JA (1980) *J Chem Phys* 72:650;
(b) Hehre WJ, Ditchfield R, Pople JA (1972) 56:2257;
(c) Boggs JE, Cordell FR (1981) *J Mol Struct* 76:329
15. (a) Flament JP (1984) *J Chim Phys* 81:673;
(b) Likas SG, Liebman JF, Levin RD (1984) *J Phys Chem Ref Data* 13:695
16. (a) Schlegel HB (1982) *J Comp Chem* 3:214;
(b) Schlegel HB (1984) *Theor Chim Acta* 66:333
17. Binkley JS, Whiteside RA, Krishnan R, Seeger R, Defrees DI, Shlegel HB, Topiol S, Kahn LR, Pople JA (1980) *QCPE* 13:406
18. Fletcher R (1980) *Practical methods of optimization*, vol. 1. Wiley, Chichester
19. Peterson MR, Poirier RA: *MONSTERGAUSS*, Department of Chemistry, University of Toronto, Canada
20. Miertuš S, Scrocco E, Tomasi J (1981) *Chem Phys* 55:117
21. Hehre WJ, Lathan WA, Ditchfield R, Newton MD, Pople JA (1973) *QCPE* 11:236
22. Bonaccorsi R, Palla P, Tomasi J (1984) *J Am Chem Soc* 106:1945
23. In a typical calculation, no more than 10 points were skipped due to this safeguard
24. Pierotti RA (1976) *Chem Rev* 76:717
25. Halicioglu T, Sinanoglu O (1969) *Ann NY Acad Sci* 158:308
26. Hirschfelder JO, Stevenson PP, Eyring H (1937) *J Chem Phys* 5:896
27. Bondi A (1954) *J Phys Chem* 58:929
28. Dugben AJ, Miertus S (1982) *Chem Phys Lett* 88:395
29. Huron MJ, Claverie P (1972) *J Phys Chem* 76:2123
30. Miertus S, Tomasi J (1982) *Chem Phys* 65:239
31. Bonaccorsi R, Cimraglia R, Tomasi J (1983) *Chem Phys Lett* 99:77
32. Moelwyn-Hughes EA 1965 *Physical chemistry*. Pergamon Press, Oxford
33. BATTERY RG, Ling LC, Guadagni DG (1969) *J Agro Food Chem* 17:385
34. Cabani S, Gianni P, Mollica V, Lepori L (1981) *J Solution Chem* 10:563
35. Spangler D, Williams IH, Maggiora GM (1983) *J Comput Chem* 4:524
36. (a) Clavero C, Lledós A, Durán M, Ventura ON, Bertrán J (1986) *J Am Chem Soc* 108:923;
(b) Clavero C, Lledós A, Durán M, Ventura ON, Bertrán J *J Comput Chem*: to be published
37. Rodwell WR, Bouma WJ, Radom L (1980) *Int J Quantum Chem* 18:107
38. *Interatomic Distances Supplement*, Esp. Publ. No 18, Chem Soc, London, 1965
39. Harmony MD, Laurie VW, Kuezkowski RL, Schwendeman RH, Ramsay DA, Lovas FJ, Lafferty WJ, Maki AG (1979) *J Phys Chem Ref Data* 8:619
40. Symons MCR (1980) *J Am Chem Soc* 102:3982
41. Blank B, Fischer H (1973) *Helv Chim Acta* 56:506
42. Kilb RW, Lin CC, Wilson Jr EB (1957) *J Chem Phys* 26:1695
43. Pascual Ahuir JL, Silla E, Tomasi J, Bonaccorsi R: to be published